Modal parameters identification and modeshapes reconstruction for CFRP panels with operational modal analysis performed with Digital Image Correlation

1st Nicola Russo
Industrial Engineering Department
University of Naples Federico II
Via Claudio 21, 80125 Napoli, Italy
nicola.russo4@unina.it

2nd Lorenzo Esposito
Industrial Engineering Department
University of Naples Federico II
Via Claudio 21, 80125 Napoli, Italy
lorenzo.esposito2@unina.it

3rd Ernesto Monaco
Industrial Engineering Department
University of Naples Federico II
Via Claudio 21, 80125 Napoli, Italy
ermonaco@unina.it

***Abstract*—This paper explores the possibility of implementing a CFRP panel defect identification procedure by performing an Operational Modal Analysis using a contactless procedure. Traditional operational and experimental modal analysis techniques imply using accelerometers mounted directly on the structure and excitations provided directly on the structure with instrumented hammers or shakers. These components introduce non-negligible impacts in the case of highly flexible structures with intrinsic low stiffness. The project's main idea is to provide the CFRP panel with a broadband white noise excitation employing a conic loudspeaker. The response of the structure will be measured with Digital Image Correlation techniques. To extract modal parameters and reconstruct structure mode shapes, we have developed software that runs Operational Modal Analysis algorithms based on the SSI-COV method for system identification. Given the setup above, it will be possible to carry out operational modal analysis with a noninvasive technique, allowing surface deformations to be measured without altering the structural integrity or the performance of the object under examination.**

***Index Terms*—CFRP panel, Operational Modal Analysis, Covariance-Driven Stochastic Subspace Identification, Digital Image Correlation,**

I. Material and methods

This section offers an overview of Digital Image Correlation (**DIC**) and Covariance-driven Stochastic Subspace Identification (**COV-SSI**), the two primary techniques used in this paper to implement a contactless procedure for modal parameter extraction and modeshape reconstruction of a CFRP plate under broadband acoustic and impulse excitation. We will cover both the general aspects and theoretical formulation of these methods.

A. Digital Image Correlation

Testing can generally be conducted using either contact sensors (e.g., accelerometers or strain gauges) or optical methods. Contact sensors offer lower computational costs and are well-suited for high-frequency data acquisition due to their relatively simple configuration. However, they provide only localized measurements, which can be affected by errors induced by the added mass or stiffness of the measuring instrument. Additionally, the necessity of wiring introduces electrical noise and limits the testing of rotating structures [29].

To overcome these limitations, various optical measurement techniques have been developed [23]. Examples include the laser Doppler vibrometer (LDV), which measures vibration velocity based on Doppler frequency shifts; electronic speckle pattern interferometry (ESPI), an interferometric technique that uses laser illumination to generate speckle patterns and detects surface displacements by analyzing interference fringes between images captured under different loading conditions; and shearography, which measures surface strain gradients by analyzing phase shifts in laser light reflections. Another widely used technique is Digital Image Correlation (DIC), a non-contact, full-field optical method capable of capturing complex structural behavior under dynamic excitation [26], [27].

First introduced by Sutton et al. in 1983 [30], DIC has been extensively applied in aerospace engineering. It operates across scales, from micro to macro, making it well-suited for full-field inspection of large structures [24]. The method involves recording a sequence of images of a speckled surface using cameras. A region of interest (ROI) is manually selected and divided into an evenly spaced virtual grid, where each subset is tracked to compute displacements and derive full-field deformation data [28]. By analyzing the speckle pattern, DIC software reconstructs the deformed shape, enabling dynamic evaluation of deflections and strains throughout the test duration.

The use of a stereo camera configuration allows for out-of-plane deformation measurements, a technique commonly referred to as 3D volumetric digital image correlation (VDIC)

or 3D DIC [31]. In this study, a 3D DIC technique is employed.

B. Operational Modal Analysis

The CFRP panel has been exposed to an impact excitation and subjected to an acoustic white noise signal to avoid mechanical contact between the specimen and the excitation. Operational Modal Analysis represented an intriguing technique for modal parameter identification and mode shape reconstruction in this framework [18] [12] [7] [6]. Operational Modal Analysis is an output-only method that allows the extraction of structural modal parameters, such as natural frequency and modal damping, based solely on vibration data collected in operating conditions [1] [2] [11]. Generally speaking, **OMA** algorithms are deployed when the structure cannot be artificially excited due to its dimensions [16] [17] [19] [20]. **OMA** algorithms can be divided into two main categories [17]:

- Frequency domain algorithms such as the Peak Peaking Method (**PP**) or the Frequency Domain Decomposition (**FDD**)
- Time Domain algorithms such as Stochastic Subspace identification with its data or covariance-driven methods (**DATA-SSI**, **COV-SSI**), the Time Domain Decomposition (**TDD**) or the Auto-regressive moving average (**ARMA**).

Given its high accuracy concerning modal parameter estimation and good computational efficiency, The Covariance-driven Stochastic Subspace Identification Method (**COV-SSI**) was chosen despite its complex mathematical formulation [8] [10] [14] [15] [21] . Let us consider a linear multi-degree of freedom system described with the following equation:

$$\mathbf{M}\ddot{x}(t) + \mathbf{C_d}\dot{x}(t) + \mathbf{K}x(t) = f(t) \tag{1}$$

- $\mathbf{M}$ is the mass matrix
- $\mathbf{C_d}$ is the damping matrix
- $\mathbf{K}$ is the stiffness matrix
- $x(t)$ is the displacement vector
- $f(t)$ is the excitation force

The second order system equation 1 can be simplified to a first order equation system which can be written in matrix form as:

$$\begin{cases} \mathbf{x}_{k+1} = \mathbf{A}\mathbf{x}_k + \mathbf{w}_k \\ \mathbf{y}_k = \mathbf{C}\mathbf{x}_k + \mathbf{v}_k \end{cases} \tag{2}$$

- y_k is the discrete output vector
- x_k is the discrete state vector
- $\mathbf{A}$ is the state transition matrix
- $\mathbf{C}$ is the output matrix
- w_k is the process noise
- v_k is the measurement noise

Notice that w_k and v_k represent the process and the measurement noise vector due to modeling and measurement error. They are assumed as zero mean white noises with the following covariance matrix:

$$E\left[\begin{pmatrix} w_p \\ v_p \end{pmatrix}\begin{pmatrix} w_q^\top & v_q^\top \end{pmatrix}\right] = \begin{pmatrix} \mathbf{Q} & \mathbf{S} \\ \mathbf{S}^\top & \mathbf{R} \end{pmatrix}\delta_{pq} \tag{3}$$

The first step to identify the modal parameters from the state transition matrix $\mathbf{A}$ is determining the covariance matrix given by

$$R_i = E\left[y_{k+i}y_k^\top\right] = \lim_{N\to\infty}\frac{1}{N}\sum_{k=0}^{N-i} y_{k+i}y_k^\top \tag{4}$$

- y_k is a vector of sensor measurements with its dimension
- k the time index
- i is the time lag
- N is the data sample

The covariance matrices can be formed into a Hankel or Toeplitz matrix, which can be decomposed with a Singular Value Decomposition (SVD)

$$\mathbf{H} = \mathbf{U}\Sigma\mathbf{V} \tag{5}$$

- $\mathbf{U}$, $\mathbf{V}$ are orthogonal matrices of left and right singular vectors
- $\mathbf{\Sigma}$ is a diagonal matrices of singular values

Given the SVD decomposition of the Hankel covariance matrix, system parameters can be retrieved from system matrix and output matrix.

II. The Experimental Set-up

This section will present an overview of the experimental setup, both in terms of hardware and software. The test involved exposing the CFRP panel to direct acoustic excitation. The panel dimensions are 1200 mm × 900 mm × 25 mm and the stringers are placed with an equal spacing of 200 mm along the long side [22]. It was hung in a suspended position to emphasize global and local responses.

A. The Digital Image Correlation system

A 3D optical measurement system acquired the acceleration data called ARAMIS 3D GOM by Zeiss. It consists of:

- Two high-resolution CMOS sensors mounted on a graduated beam that allows correct alignment along the horizontal axis
- A laser pointer for sensor positioning
- Multiple LED lights to correctly illuminate the test article
- A computer to process data image

This system tracks both static and dynamic loading effects by recording time-series measurements of reference point or speckle pattern coordinates. From these measurements, it calculates displacements, strains, velocities, and accelerations. The system's temporal resolution is directly determined by the image capture frequency.

Fig. 1. CFRP panel under investigation

B. The Operational Modal Analysis Software

Software that implements the COV-SSI method has been developed to extract the structure's modal parameters and reconstruct mode shapes. The software allows you to create the panel geometry and associate the acceleration data logged along the three dimensions to each measurement point. Given that the implemented method is based on coherence, the signal can be processed to smooth data and focus the modal parameter extraction on a specific frequency range. The software allows data decimation, pass band filter application, and data segmentation. The COV-SSI method is applied to extract modal parameters for 50 model orders. The software is set to produce a stabilization diagram around stability conditions over frequency, modal damping, and mode shapes. Let us note that the number of stable poles and the frequency range are strongly affected by the chosen model order (50 poles) and are dictated by the SVD decomposition for which the singular values are ordered in terms of relative magnitude [5] .

III. The Experimental Campaign

Experimental campaign has been organized in three phases. First, an experimental modal analysis was carried out to provide a baseline for modal parameter identification and mode shape reconstruction. The excitation was provided with an instrumented hammer and the responses acquired by accelerometers. Second, we performed an operational modal analysis panel employing accelerometers as sensors and an acoustic broadband excitation provided by a wide range speakers as dynamic load. The last step consisted of performing an operational modal analysis with data retrieved by DIC employing high speed cameras as sensors. In this case, the excitation was provided with an instrumented hammer. We discretized the panel with 55 points, 30 bays and 25 stringers.

A. Experimental modal analysis

The authors performed the experimental modal analysis of the panel with the roving hammer technique. The measurement triaxial accelerometer was placed in the S29 position while the excitation was provided for each point. The FRFs along the three axes were averaged over five impacts for each excitation point. The FRFs were processed with Testlab by Siemens software to extract both modal parameters and mode shapes [9]. We chose a force (5%) - exponential (100%) window. We identified a total of 24 physical stable modes summarized in table III

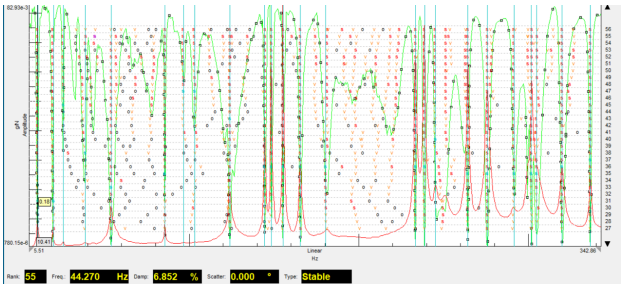

Fig. 2. EMA stabilitazion diagram

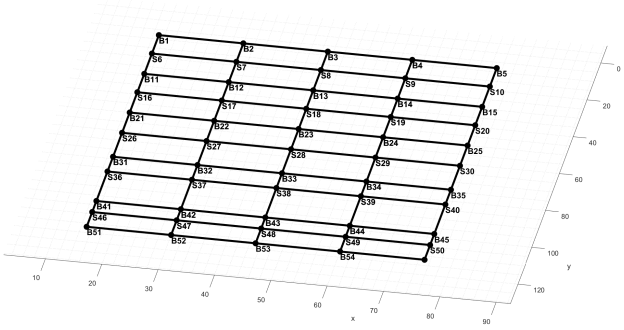

Fig. 3. Reconstructed test article geometry

B. The operational modal analysis with acoustic excitation

In the first OMA test, the provided excitation was a 30 s white noise windowed in the [50-315] Hz range. The speaker was positioned 50 cm from the panel. The reason behind the choice of the band relied on the physical characteristics of the loudspeaker, which had its impedance peak at 50 Hz and, therefore, was incapable of reproducing lower frequencies. The upper limit was set to focus the amplifier energy in the range in which main global panel modes were expected. 2 tri-axial and two mono-axial 100 mV/g accelerometers were deployed. The panel surface was covered with 19 runs; for each run, three accelerometers were scattered in bay and stringer positions, while a reference accelerometer was kept in position S29. Sampling frequency was set to 1024 Hz. Data retrieved for each run were processed using the designed

TABLE I
MODAL PARAMETER OF THE TEST ARTICLE IDENTIFIED WITH EMA

	Modal Parameter estimate for stable poles		
	Mode Number	*Frequency*	*Modal Damping %*
	1	10.66	7.08
	2	20.00	3.85
	3	25.64	5.25
	4	38.54	4.50
	5	53.98	2.41
	6	85.58	0.42
	7	96.42	2.36
	8	103.31	2.72
	9	123.81	0.57
	10	144.48	0.32
	11	148.35	0.24
	12	155.31	0.21
	13	165.50	0.43
	14	180.44	1.54
	15	233.39	0.27
	16	238.76	0.34
	17	245.29	1.32
	18	264.26	0.23
	19	275.78	0.40
	20	291.56	0.74
	21	301.84	0.24
	22	304.91	1.00
	23	319.91	0.37
	24	336.60	0.19

OMA software. For simplicity, the stabilization diagram and the modal parameters are shown only for one run. Interestingly, similar frequencies and modal damping were identified across the different runs for which accelerometers were placed almost randomly on the panel, keeping both stringers and bay points. For instance, RUN 1 was composed by points B1, S47, S20, S29 as reported in figure 7.

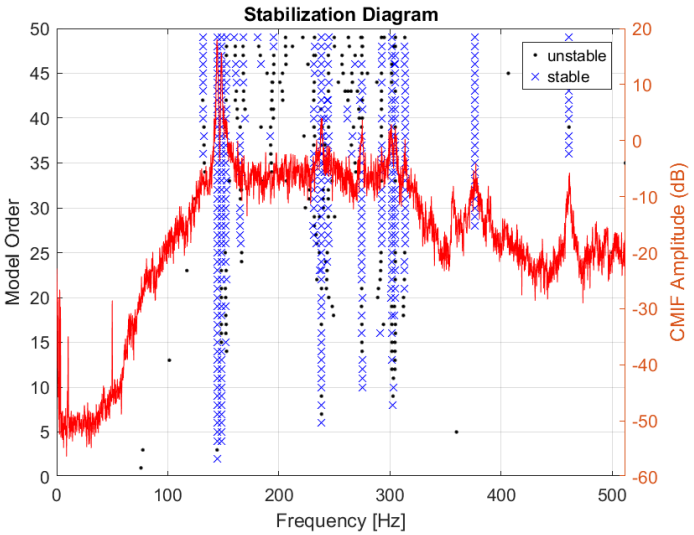

Fig. 4. OMA stabilitazion diagram - RUN1

TABLE II
MODAL PARAMETER OF THE TEST ARTICLE IDENTIFIED WITH OMA WITH ACOUSTIC EXCITATION APPROACH - RUN 1

	Modal Parameter estimate for stable poles		
	Mode Number	*Frequency*	*Modal Damping %*
	1	131.64	2.60
	2	144.45	0.27
	3	148.26	0.16
	4	152.87	0.98
	5	159.97	3.09
	6	167.67	0.49
	7	181.21	2.62
	8	195.26	-0.34
	9	238.46	0.32
	10	244.71	0.33
	11	301.63	0.20
	12	376.54	0.81
	13	461.24	0.33

C. The operational modal analysis with impact excitation and DIC retrieved data

The last task consisted of performing an operational modal analysis with data retrieved with a 3D optical system and impulsive contact excitation. Cameras were placed 1.64 m from the specimen. Given the light conditions and the dimensions of the specimen, it was possible to measure the displacements of 45 points at a maximum frequency of 300 Hz. The excitation was provided with a modal hammer. The test article has been impacted in five different points to ensure the complete excitation of the specimen; no force has been measured. For simplicity, the stabilization diagram and the modal parameters are shown only for one run Displacements were processed with the same OMA software to extract modal parameters and modeshapes.

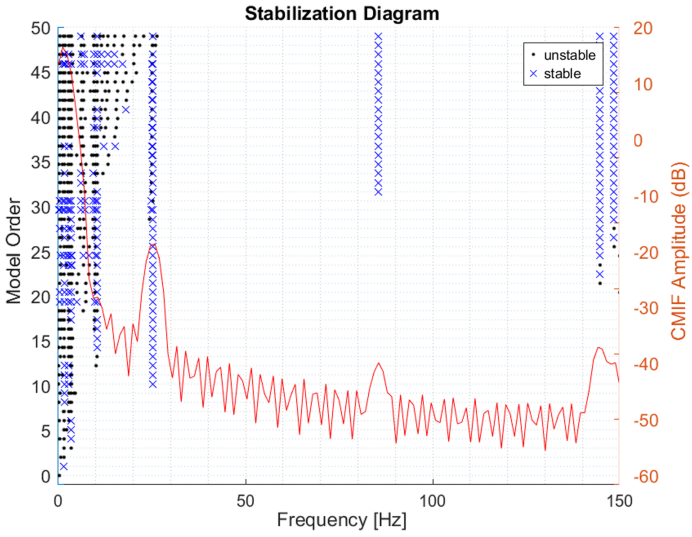

Fig. 5. OMA stabilitazion diagram for impact excitation and DIC retrieved data - RUN1

TABLE III
MODAL PARAMETER OF THE TEST ARTICLE IDENTIFIED WITH OMA (DIC APPROACH)

	Modal Parameter estimate for stable poles		
	Mode Number	*Frequency*	*Modal Damping*
	1	6.07	4.01
	2	10.34	1.35
	3	25.32	0.27
	4	85.55	0.54
	5	144.66	0.28
	6	148.46	0.21

IV. DISCUSSION

Analyzing the results of the identified modal parameters obtained with the three different techniques, excellent levels of similarity. It is evident that each method had some intrinsic criticalities given by the type of excitation or acquisition method. In the case of the OMA carried with accelerometers and acoustic excitation, the speaker did not allow any consistent excitation below 100 Hz: this implied that the first excited high-energy modes were around 144 Hz. Modes identified with this type of OMA (acoustic excitation and accelerometers) matched consistently with the one identified with the EMA approach in both frequency and damping (e.g., modes around 144 Hz, 148 Hz, 165 Hz, 244 Hz, etc.). It is interesting to notice that in the case of modal parameters and mode shapes identified with OMA with the DIC techniques and impulse excitation approach, the authors pointed out the same level of consistency with EMA in the frequency range up to 150 Hz (e.g., modes around 10 Hz, 25 Hz, 85 Hz, 144 Hz, 148 Hz). Given light conditions, it was not possible to extend the frequency range. To ensure compliance, the mode shapes reconstructed with OMA and DIC techniques were compared to the ones obtained with the EMA approach. Let us consider the two modes extracted with each approach (144 Hz and 148 Hz). It is clear that both techniques provided the same results. The authors decided to omit modeshapes reconstructed from OMA analysis with acoustic excitation due to the limited number of acquisition points for each run.

V. CONCLUSION

This work explored the possibility of performing contactless operational modal analysis with acoustic excitation and digital image correlation techniques. A preliminary experimental modal analysis of the CFRP panel has been carried out to set a baseline for modal parameter identification and modeshape reconstruction. The authors have developed an OMA software deploying the SSI-COV algorithm to process data. The second step consisted of performing an operational modal analysis of the test article excited by means of acoustic white noise produced with a conic loudspeaker. The accelerations were measured with inertial accelerometers in 19 runs of four acquired simultaneous positions each. In the frequency range in which this OMA approach overlapped with EMA, the identified modal parameters were consistent with the one of the baseline. As the third step, an OMA approach was followed, deploying displacements measured with a 3D optical system with a sampling frequency of up to 300 Hz. The excitation was impulsive. In the frequency range in which this OMA approach overlapped with EMA, modal parameters and mode shapes were highly consistent. The last step consisted of exposing the panel to acoustic excitation and measuring displacement with optics. The level of excitation provided by the actual amplifier/ loudspeaker setup and the actual light conditions did not allow for a satisfactory signal-to-noise ratio, resulting in noisy measurements of the optics. Further analyses are being done in order to validate the approach. Even if non completely contactless, both the OMA approaches resulted in coherent modal parameters and modeshape identifications. In the case of acoustic excitation, it was possible to identify the system by logging 30 seconds of acceleration data from four data points scattered along the test article. The DIC method allowed for extremely rapid testing, given the possibility of following the vast majority of the test article simultaneously. Compared to EMA, the presented OMA techniques were significantly faster yet accurate, providing a good baseline for further developments.

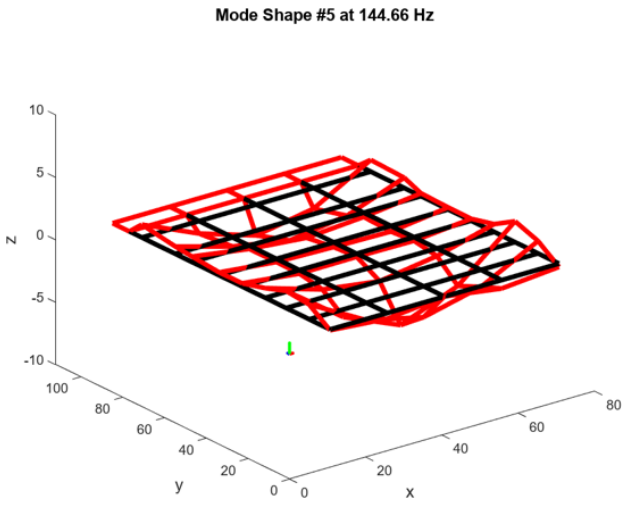

Fig. 6. Modeshape at 144,66 Hz obtained with impact excitation and DIC retrieved data

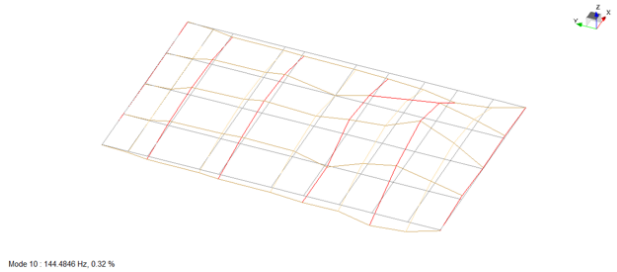

Fig. 7. Modeshape at 144,48 Hz obtained with EMA

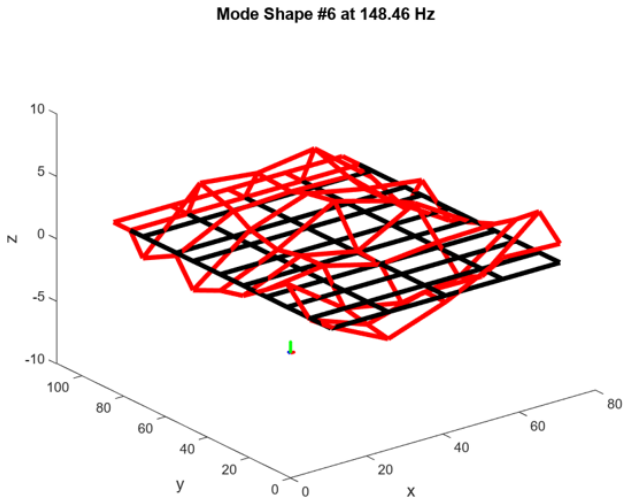

Fig. 8. Modeshape at 148,46 Hz obtained with impact excitation and DIC retrieved data

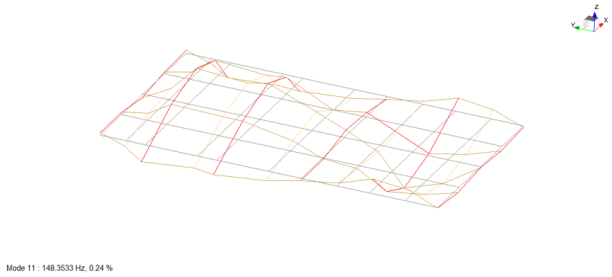

Fig. 9. Modeshape at 148,33 Hz obtained with EMA

REFERENCES

[1] F. Magalhães , Á. Cunha, E. Caetano, "Dynamic monitoring of a long span arch bridge", Engineering Structures, Volume 30, Issue 11, 2008, Pages 3034-3044, ISSN 0141-0296, https://doi.org/10.1016/j.engstruct.2008.04.020.

[2] F. Magalhães, Á. Cunha, E. Caetano, "Online automatic identification of the modal parameters of a long span arch bridge", Mechanical Systems and Signal Processing, Volume 23, Issue 2, 2009, Pages 316-329, ISSN 0888-3270, https://doi.org/10.1016/j.ymssp.2008.05.003.

[3] S. S. Saidin, S. A. Kudus, A. Jamadin, M. A. Anuar, N.i Mohd Amin, Z. Ibrahim, A. Bt Zakaria, K. Sugiura, "Operational modal analysis and finite element model updating of ultra-high-performance concrete bridge based on ambient vibration test", Case Studies in Construction Materials, Volume 16, 2022, e01117, ISSN 2214-5095,

[4] H. Pan, Y. Li, T. Deng, J. Fu, "An improved stochastic subspace identification approach for automated operational modal analysis of high-rise buildings", Journal of Building Engineering, Volume 89, 2024, 109267, ISSN 2352-7102,

[5] D.P. Pasca, A. Aloisio, M. M. Rosso, S. Sotiropoulos. "PyOMA and PyOMA_GUI: A Python module and software for Operational Modal Analysis" . SoftwareX. 10.1016/j.softx.2022.101216. 2022

[6] F. Bin Zahid, O. Chao, S. Khoo. "A review of operational modal analysis techniques for in-service modal identification". Journal of the Brazilian Society of Mechanical Sciences and Engineering. 42, 2020, 10.1007/s40430-020-02470-8.

[7] B. Peeters. "System Identification and Damage Detection in Civil Engineering". 2020

[8] B. Peeters, G. De Roeck. "Stochastic System Identification for Operational Modal Analysis: A Review". Journal of Dynamic Systems Measurement and Control-transactions of The Asme - J DYN SYST MEAS CONTR. 123. 2002 10.1115/1.1410370.

[9] B. Peeters, H. Van der Auweraer. "PolyMax: a revolution in operational modal analysis". 1st International Operational Modal Analysis Conference. 2005

[10] B. J. O'Connell, T. J. Rogers, "A robust probabilistic approach to stochastic subspace identification", Journal of Sound and Vibration, Volume 581, 2024, 118381, ISSN 0022-460X.

[11] C. Rainieri, G. Fabbrocino, "Operational Modal Analysis of Civil Engineering Structures", 2014, doi:10.1007/978-1-4939-0767-0

[12] E. Reynders, "System Identification Methods for (Operational) Modal Analysis: Review and Comparison". Archives of Computational Methods in Engineering. 19. 51-124, 2012, doi: 10.1007/s11831-012-9069-x.

[13] K. Cho, J. R. Cho. "Stochastic Subspace Identification-Based Automated Operational Modal Analysis Considering Modal Uncertainty". Appl. Sci. 2023, 13, 12274.

[14] S. Chauhan. "Subspace Algorithms in Modal Parameter Estimation for Operational Modal Analysis: Perspectives and Practices". De Clerck, J., Epp, D. (eds) Rotating Machinery, Hybrid Test Methods, Vibro-Acoustics & Laser Vibrometry, 2016, Volume 8. Conference Proceedings of the Society for Experimental Mechanics Series. Springer, Cham. https://doi.org/10.1007/978-3-319-30084-9_27

[15] R. Brincker,P. Andersen. "Understanding Stochastic Subspace Identification". 2006

[16] B. Peeters, G. Couvreur, O. Razinkov, C. Kündig, H. Van der Auweraer, G. De Roeck. "Continuous monitoring of the Øresund Bridge: System and data analysis". Structure and Infrastructure Engineering - STRUCT INFRASTRUCT ENG. 5. 2009. 10.1080/15732470701478362.

[17] H. Hasani, F. Freddi, "Operational Modal Analysis on Bridges: A Comprehensive Review". Infrastructures 2023, 8, 172. https://doi.org/10.3390/infrastructures8120172.

[18] R. Brincker, C. Ventura. Introduction to Operational Modal Analysis. 10.1002/9781118535141. 2015.

[19] B. Peeters, F. Dammekens, F. Magalhães, H. Van der Auweraer, E. Caetano, Elsa, A. Cunha. "Multi-run Operational Modal Analysis of the Guadiana cable-stayed bridge".

[20] B. Peeters, F. Vanhollebeke, H. Van der Auweraer. "Operational Modal Analysis for Estimating the Dynamic Properties of a Stadium Structure during a Football Game". Shock and Vibration. 14. 2007. 10.1155/2007/531739.

[21] P. Van Overschee, B. De Moor. "Subspace Identification for Linear Systems". 1996, 10.1007/978-1-4613-0465-4_2.

[22] V. Memmolo, E. Monaco, N.D. Boffa, L. Maio, F. Ricci, "Guided wave propagation and scattering for structural health monitoring of stiffened composites", Composite Structures, Volume 184, 2018, Pages 568-580, ISSN 0263-8223,

[23] J. Baqersad, P. Poozesh, C. Niezrecki, P. Avitabile. "Photogrammetry and optical methods in structural dynamics – A review". Mechanical Systems and Signal Processing. 86. 2016 10.1016/j.ymssp.2016.02.011.

[24] W. Broughton. Testing the Mechanical, "Thermal and Chemical Properties of Adhesives for Marine Environments". 2012. 10.1016/B978-1-84569-452-4.50006-0.

[25] D. Zhang, C. D. Eggleton, D. Arola. "Evaluating the mechanical behavior of arterial tissue using digital image correlation". Experimental Mechanics, 42(4), 409-416. 2002, https://doi.org/10.1007/bf02412146

[26] B. Mastrodicasa, C. Ferreira, B. Peeters, M. Vaz, P. Guillaume. "DIC Using Low Speed Cameras on a Scaled Wind Turbine Blade". 2022, 10.1007/978-3-031-04098-6_2.

[27] D. Mastrodicasa, L. Wittevrongel, P. Lava, B. Peeters. "Full-Field Modal Analysis by Using Digital Image Correlation Technique". 2020, 10.1007/978-3-030-47721-9_15.

[28] B. Mobasher, "Textile fiber composites: Testing and mechanical behavior", Thanasis Triantafillou, Textile Fibre Composites in Civil Engineering, Woodhead Publishing, 2016, Pages 101-150, ISBN 9781782424468,

[29] P. Poozesh, A. Sabato, A. Sarrafi, C. Niezrecki, P. Avitabile. "A multiple stereo-vision approach using three dimensional Digital Image Correlation for utility-scale wind turbine blades". 2018.

[30] M. Sutton, W. Wolters, W. Peters, W. Ranson, S. McNeill, "Determination of displacements using an improved digital correlation method", Image and Vision Computing, Volume 1, Issue 3, 1983, Pages 133-139, ISSN 0262-8856,

[31] M. Sutton, J. Orteu, H. Schreier, "Image correlation for shape, motion and deformation measurements: basic concepts, theory and applications", Ed. Springer Science & Business Media, 2009,